AIChE

Modeling and Parametric Analysis of Hollow Fiber Membrane System for Carbon Capture from Multicomponent Flue Gas

Rajab Khalilpour and Ali Abbas
School of Chemical and Biomolecular Engineering, The University of Sydney, Sydney, Australia

Zhiping Lai and Ingo Pinnau
Advanced Membranes and Porous Materials Center KAUST, Thuwal, Saudi Arabia

DOI 10.1002/aic.12699
Published online August 12, 2011 in Wiley Online Library (wileyonlinelibrary.com).

The modeling and optimal design/operation of gas membranes for postcombustion carbon capture (PCC) is presented. A systematic methodology is presented for analysis of membrane systems considering multicomponent flue gas with CO_2 as target component. Simplifying assumptions is avoided by namely multicomponent flue gas represented by CO_2/N_2 binary mixture or considering the co/countercurrent flow pattern of hollow-fiber membrane system as mixed flow. Optimal regions of flue gas pressures and membrane area were found within which a technoeconomical process system design could be carried out. High selectivity was found to not necessarily have notable impact on PCC membrane performance, rather, a medium selectivity combined with medium or high permeance could be more advantageous. © 2011 American Institute of Chemical Engineers *AIChE J*, 58: 1550–1561, 2012
Keywords: carbon capture, membrane, multicomponent gas, modeling, parametric analysis

Introduction

Avoiding CO_2 emissions is seen as imperative, and governments have recognized this as a key objective toward curbing effects of extreme weather, higher temperatures, worsening droughts and floods, and rising sea levels. Fossil fuels are the main contributors for CO_2 emissions. As such, carbon capture and storage (CCS) is viewed as a solution and a bridge from the current fossil fuel-based energy system to one that has near-zero carbon emissions.

The premier interest in implementation of CCS projects is the large CO_2 sources, e.g., power plants accounting for about 78% of worldwide large stationary CO_2 sources.[1] There are three main approaches to capturing CO_2 from power plants; precombustion, oxyfuel combustion and postcombustion. Comprehensive descriptions of these processes can be found elsewhere.[2–3] Although oxyfuel and precombustion technologies are studied extensively to be applied into new-build power plants, postcombustion (PCC) may be the most accessible option for retrofitting existing power plants due to minimum changes required to the existing plant.[4]

A few technologies have been discussed for PCC; i.e., solvent-based absorption-desorption,[5] membrane, adsorption[6–7] and mineralization.[8] Solvent-based PCC although being the best available technology (BAT), is not a long-term desired technology for PCC due to its high-energy penalty for solvent regeneration.[5]

Membrane-based PCC (MPCC) is one of the technologies that may have good potential to compete with solvent technology although currently being under very controversial discussions. The main advantages of membrane separation over other technologies include compactness, modularity, and ease of installation by skid-mounting, ability to be applied in remote areas such as offshore, flexibility in operation and maintenance and in most cases lower capital cost as well as lower energy consumption.[9]

Carbon dioxide separation using membranes is widely addressed in the context of natural gas sweetening where the gas coming from the well contains CO_2 and H_2S and is required to be reduced to pipeline specifications ($CO_2 = 2\%$ and $H_2S = 4$ ppm).[10–11] However, this does not necessarily certify the practicality of using membranes for separation of CO_2 from flue gas due to the CH_4-CO_2 and CO_2-N_2 systems having differences in selectivity and in molecular size ratios of the binary components as well as due to different impacts of adsorption or capillary condensation effects.

The pioneer work on CO_2/N_2 separation may be traced back to the article by Kawakami et al.[12] They studied the impact of blending a low-permeable glassy polymer (cellulose nitrate) with a plasticizer membrane (poly (ethylene glycol), PEG) on CO_2/N_2 separation. The interesting point of this research was that the authors did not have clear ideas for industrial applications of CO_2/N_2 separation and only projected that the separation of CO_2 from N_2 might be used "in order to recover carbon resources or to control CO_2 concentration in an artificial atmosphere".

It was mainly after the United Nation's Earth Summit, held June 1992 in Brazil, that researches on different alternative approaches, including membrane, for separation of CO_2 from flue gas (PCC) accelerated due to the high-commercial value forecast. Since then various researches

Correspondence concerning this article should be addressed to A. Abbas at ali.abbas@sydney.edu.au.

© 2011 American Institute of Chemical Engineers

have been carried out on membrane material design (MMD) and membrane systems engineering (MSE) specifically for separation of CO_2 from flue gas.

The review of studies on MMD is out of the context of this study. In a detailed study, Powell and Qiao[13] reviewed available membrane materials for flue gas separation, possible design strategies, synthesis, fabrication and role of novel materials. Their survey included a number of different classes of polymers as well as carbon and mixed matrix membranes. Their survey which covered some 190 reports concluded that copolymers and polymer blends had higher potential for further research.

It is currently observed that most of the studies on CO_2 capture membranes are focused on improving selectivity and literature lacks proper attention to other important requirements such as stability, resistance to high pressure, useful lifetime, and so on. The other gap in the literature is ignoring the impact of other components of flue gas such as water vapor, O_2, CO_2, SO_x, NO_x, NH_3, etc. With few exceptions,[14–16] all prior studies focus on a binary mixture of N_2 and CO_2. Most of the available selectivity values are for this binary mixture.

Understanding the important role of minor components in the design and operation of membranes for carbon capture, Scholes et al.[17] reviewed those polymeric membranes considering impact of minor gases on membrane permeability, plasticization and aging effects. Their conclusion was that "while many minor components can affect performance both through competitive sorption and plasticization much remains unknown. This limits the selection process for membranes in this application". One of the examples of this type is the recent study of Merkel et al.[14] who highlighted the beneficial effect of water vapor in PCC. This is while, it has been traditionally thought that water, due to having higher permeability than CO_2 and due to solubility of CO_2 in water, will cause plasticization effect and also Scholes et al.[15] very recently, reported negative impact of water.

Even in significant portion of studies, permeability of each pure gas N_2 and CO_2 over the membrane is experimentally analyzed and then CO_2/N_2 selectivity is obtained by division of the two values. This is while it is a general consensus that permeability of a gas at pure and at mixture conditions is very different due to different molecules' competition in diffusion and sorption.[18] An analogy can be drawn with thermodynamics, the first approach could be called "ideal" selectivity and the latter "real". Therefore, future studies should first place effort in producing real selectivity values for CO_2/N_2 mixtures, and the second attempt to use realistic flue gas compositions at least while considering oxygen and water vapor.

We can, therefore, conclude from this review that research in the field of MMD is mainly focused on improving the permselectivity of CO_2/N_2 and other attributes of a proper membrane, i.e., stability and compatibility, while influence and considerations of the real process environment and operational parameters are not explored well yet.

Another series of studies have focused on MSE. Vandersluijs et al.[19] in an economical study, investigated the feasibility of polymer membranes for the recovery of CO_2 from flue gases of a power plant. They presented a cross-flow permeation model and used optimization to determine CO_2 abatement costs. They pointed out that with the membranes available at the time of their study, MPCC could not compete with solvent-based technologies. They proposed that for membranes to become economically attractive for carbon capture, membranes with CO_2/N_2 selectivity higher than 200 along with high permeability would be required. The value of selectivity of 200 has thereafter been widely accepted and/or cited by various publications.[20–23] According to Kazama et al.[24] the total cost of amine process is even cheaper than a cardo polyimide hollow fiber membranes with CO_2/N_2 selectivity of 40 and having high CO_2 permeance of 1,000 GPUs. They estimated that in the CO_2 concentration range above 25%, membrane systems become advantageous over other technologies.

Matsumiya et al.[25] having concern about energy consumption for the separation of CO_2 in the flue gas used two different scenarios for achieving required driving force between feed and permeate side. In one scenario they compressed flue gas while the permeate side was under atmospheric pressure. In the other approach they used flue gas in its natural atmospheric pressure but made vacuum condition in downstream permeate side. They noticed that the energy consumption required for achieving the driving force using the vacuum strategy was significantly less than the one with compression.

Bounaceur et al.[26] assuming the flue gas as a binary mixture of CO_2 and N_2 and using cross-plug flow model inside a single-stage membrane compared the feasibility of membrane against that of amine solvent process. The study concluded that with the available membranes of the time having CO_2/N_2 selectivities less than 50, the membrane process was not feasible and values above 100 were required. Another study in the same year claimed that MEA-based technology is less expensive than membrane technology even for CO_2 purity requirements as low as 60%.[27] The same conclusion was reported elsewhere.[28] Till this stage there was general consensus on infeasibility of MPCC for power plants although the quantitative values for feasibility thresholds were different for various studies. However, after this some new studies have contradicted the infeasibility idea.

Favre[21] debated the general consensus that solvent absorption technologies are more feasible than membranes. The article criticized the IPCC statement[1] on inappropriateness of membranes as being based on either incomplete or unclear arguments. According to that author, the potential of dense polymeric membranes to solve the flue gas treatment problem may have been underestimated. Ho et al.[29] with similar idea to others[25–26] compared membranes with compression against *in vacuo* scenarios for a flue gas from a coal-fired power-plant. They showed that while vacuum strategy required relatively high membrane area, it could achieve 35% less capture cost per tonne CO_2 avoided compared with compression systems. However, the conclusion was that no available membrane could result in capture cost competitive with amines.

Merkel et al.[14] reported their development of a new membrane with CO_2 permeances of greater than 1,000 GPUs and a CO_2/N_2 selectivity of 50 at 30 $^{\circ}$C which according to them has permeance 10 times higher than commercial CO_2 membranes and selectivity in the range of the highest reported for nonfacilitated transport materials. They simulated two-stage membranes with vacuum pumps and using combustion air as sweep flow. The study claimed that the membrane process can capture 90% of CO_2 in flue gas as a sequestration-ready supercritical fluid using about 16% of plant's energy at a cost as low as \$23/tonne CO_2. This suggested the feasibility of MPCC.

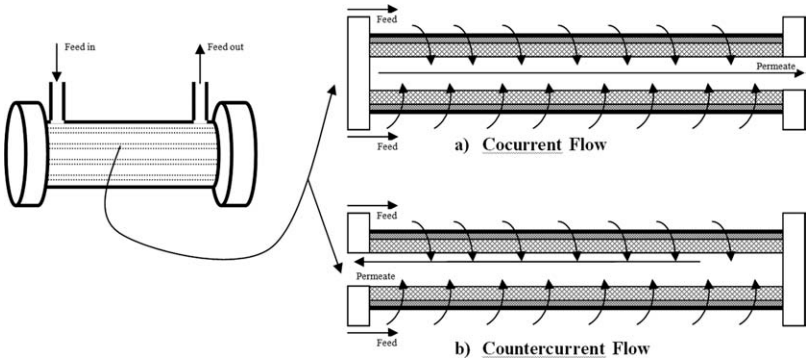

Figure 1. Schematic of hollow fiber membrane module with (a) cocurrent, and (b) countercurrent flow arrangement.

Bernardo et al.[30] in a detailed review of state-of-the-art membranes for gas separation point-out the fact that the concept of membranes application for PCC is not fully explored and "significant design optimization would be required to identify efficient, feasible, and environmentally sound technical solutions".

In our agreement with Bernardo et al.[30] one of the main problems of current studies on membrane carbon capture is the lack of proper membrane process models to be used. Most of the studies assume the flues gas as a binary mixture (CO_2 and N_2) which is not an acceptable simplification. There are some other studies that assume mixed-flow pattern which is subject to error as in reality cocurrent or countercurrent flow are used. Hollow fiber types have also undoubtedly proved to be the best at least for gas separation. We have identified a notable lack in the literature in systematic engineering analysis of membrane systems in any type of gas separation including carbon capture.[31]

In this study, we introduce our previously discussed membrane gas separation simulation algorithm,[31] implement it for single-stage membrane carbon capture and evaluate the potential of membranes in this application. The model is first presented in the following section and then its solution is presented in the other section considering both concurrent and countercurrent flow pattern hollow fiber membranes. This model has potential for identifying the optimal operating conditions (e.g., pressure) and design parameters (e.g., area). We have also presented results from a detailed parametric analysis with discussions on the interaction between various parameters as well as on the regions of optimality. Finally, conclusions are presented summarizing key findings and discussing the merits of multistage configurations as well as the value of this modeling approach in feasibility analysis of MPCC for global decision-makers in the field of carbon capture.

Multicomponent Gas Membrane Modeling

Modeling

The overall mass transfer across the membrane for any component i could be formulated as

$$N_i = \frac{\Delta F_{fi}}{A} = \frac{P_{fbi} - P_{pbi}}{R} \tag{1}$$

where N_i is mass-transfer flux of component i, ΔF_{fi} is the feed flow rate passing through the membrane, A is membrane area, P_{fb} and P_{pb_i} are bulk partial pressures of feed and permeate for component i, respectively, and R is overall mass-transfer resistance. The overall mass-transfer resistance (R) is described as a combination of three resistances (1) feed side (external) boundary layer, (2) membrane structure, and (3) the permeate side (internal) boundary layer. However, in the case of low-permeance polymer membranes for gas separation that follow solution-diffusion mechanism, permeance is the controlling parameter, and the internal/external mass-transfer resistances might be relatively negligible. This simplifies Eq. 1 to

$$\Delta F_{f_i} = A\frac{\bar{P}_i}{l_m}(P_{f_i} - P_{p_i}) \tag{2}$$

where $\bar{P}_i$ is permeability of component i over the membrane, l_m is membrane thickness and $\bar{P}_i/l_m$ is permeance (K_{m_i}). Four parameters affect mass transfer across the membrane; membrane area, thickness, permeability, and gas pressure. A successful membrane separation process, thus, requires proper values of these parameters from which two of them (thickness and permeability) are related to membrane synthesis while the other two (gas pressure and membrane area) are defined by membrane or system design.

Besides thermodynamic and mass-transfer properties, membrane module design and flow patterns also affect membrane separation.[32] There are four main types of membrane designs, i.e., flat (plate-and-frame), tubular, spiral-wound and hollow-fiber. The latter is receiving increasing attention (especially for gas separation) due to its high-packing density as a result of higher area per volume.[9] Five flow patterns have also been studied, i.e., one-side-mixing, perfect mixing, cross flow, cocurrent and countercurrent flow,[32–33] while for hollow fiber systems the practical options are cocurrent and countercurrent flows (Figure 1).

In this study, we consider hollow fiber membrane design and aim to study performance of both cocurrent and countercurrent flow patterns borrowing the idea from Pan.[34] Figure 1 illustrates a hollow fiber membrane with feed in shell-side and permeate in lumen-side. This will be our base-case model although there is not much difference when feed is inside lumen and permeate diffuses to shell-side. The key assumptions of this modeling are:

1 Permeabilities of gas components are assumed to be independent of pressure.

2 Feed-side pressure drop is assumed to be negligible.

3 Permeate pressure-drop follows the highly accepted Hagen-Poiseuille equation.[35]

The overall mass balance is given by

$$\left.\begin{array}{c} F_f + F_p = F_{f0} \\ x_i F_f + y_i F_p = x_{i0} F_{f0} \end{array}\right\} y_i = \frac{x_{i0} F_{f0} - x_i F_f}{F_{f0} - F_f} \tag{3}$$

where F_f and F_p are feed and permeate flow rates, respectively. Accordingly, x_i and y_i are molar fraction of component i in feed and permeate. The subscript 0 refers to feed condition at membrane inlet.

Following Eq. 2, the permeation rate of gas component i as well as total gas permeation through the membrane is given by Eqs. 4 and 5, respectively

$$\frac{d(x_i F_f)}{dz} = -2\pi R_o L N K_{m_i} (x_i P_f - y_i P_p) \tag{4}$$

$$\frac{dF_f}{dz} = -2\pi R_o L N \sum_1^C K_{m_i} (x_i P_f - y_i P_p) \tag{5}$$

where R_o, L and N are outer radius, length and total number of hollow fiber membrane, respectively. For a feed with C components, a set of C equations for (4) should be solved simultaneously. However, as it is noticed the ODE contains a term $x_i F_f$ where both x_i and F_f are variables over hollow fiber length. Therefore, the following equation requires further simplification

$$\frac{dx_i}{dz} = \frac{-1}{F_f}\left(2\pi R_o L N K_{m_i} (x_i P_f - y_i P_p) + x_i \frac{dF_f}{dz}\right) \tag{6}$$

for both feed and permeate sides, the following conditions should be, respectively satisfied

$$\sum_{i=1}^{C} x_i = 1 \tag{7}$$

$$\sum_{i=1}^{C} y_i = 1 \tag{8}$$

The next step is to define an equation for calculation of permeate component fraction y_i. Given $d(x_i F_f) = y_i dF_f$ combination of Eqs. 4 and 5 results in the desired Eq. 9

$$y_i = \frac{K_{m_i} x_i \sum_1^C \left(y_i / K_{m_i}\right)}{1 - \beta + \beta K_{m_i} \sum_1^C \left(y_i / K_{m_i}\right)} \tag{9}$$

In which β is the pressure ratio of permeate over feed (P_p/P_f). Pressure drop in the permeate side is defined from Hagen-Poiseuille equation

$$\frac{dP_p}{dz} = \frac{\pm 8 R T L \mu_m (F_{f_0} - F_f)}{\pi R_{in}^4 N P_p} \tag{10}$$

where R is ideal gas constant, T is temperature, μ_m is gas mixture viscosity, and R_{in} is hollow fiber inner radius. Equation 10 carries positive and negative signs for cocurrent and countercurrent flows, respectively.

The important parameter in Eq.10 requiring attention is viscosity, which varies as the concentration of permeate (and feed) changes through the fiber length. We have used the well-known Wilke[36] equation which is proved to predict multicomponent gas viscosities within an average error of 2%.

Solution algorithm

Considering the gas flow has C components ($i = 1, 2,\ldots, C$), we want to obtain the concentration profile of both feed (x_i) and permeate (y_i) over the hollow fiber length. The profiles of feed-gas flow rate and permeate pressure are also required. The profile of feed-gas pressure is not required to be calculated as we assumed it not to change over the fiber length. Permeate flow rate calculation is also redundant as by having feed-gas flow rate profile, it could be easily obtained using mass balance Eq. 3. Therefore, we have $2C + 2$ unknowns. The same number of equations is required to solve the problem. Equations 5, 6, 9 and 10 are candidate equations. These equations form a system of nonlinear differential-algebraic equation (NDAE). To solve this problem, we convert the ODEs into algebraic equations using backward finite differential equations over j segments ($j = 1, 2,\ldots, J$) of the fiber and then solve the new set of equations, all algebraic, using Gauss-Seidel algorithms.

The solution algorithm for countercurrent flow has a small difference due to the reverse direction of permeate. In cocurrent flow, both the feed and permeate initial values start at $j = 0$; the values of other segments j are then calculated step by step. However, in the case of countercurrent flow we do not have permeate pressure at $j = 0$ ($P_{p,0}$) and instead we have $P_{p,j}$. In this condition the numerical solution will have one extra iteration loop and, hence, will be more time-consuming.

Solution Output

For solution of the model, we considered a flue gas containing four components, N_2, CO_2, O_2 and H_2O at different operating conditions. Finding permselectivity data was a difficult task due to almost complete lack of such experimental data for a membrane using flue gas with more than two components. Sada et al.[16] presented experimental permselectivity data for three components of CO_2, N_2 and O_2. However, the data are out of date with low CO_2/N_2 selectivity of 15.65. Recently Merkel et al.[14] used a commercial membrane with selectivity values of 50, 2.5 and 100 for CO_2/N_2, O_2/N_2 and H_2O/N_2, respectively. We used these data as base-case in our simulation work.

The model was solved using MATLAB R2009a on a PC with 2-quad CPU of 2.83 GHz and 4 GB of RAM. Figure 2 illustrates the program output for flue gas with 13% CO_2 and pressure of 10 bar.

The permeate concentration profile is the benchmark for membrane evaluation or selection of flow pattern and other design factors. Figure 2a illustrates the CO_2 concentration (molar fraction) in permeate for cocurrent and countercurrent flows. The flow pattern can be observed to have important impact on permeate purity. While the outlet CO_2 concentration of permeate for cocurrent flow is 0.40, the corresponding value for countercurrent flow is 0.57. The permeate concentration of N_2, O_2 and H_2O will, respectively be 0.43, 0.04 and 0.13 for cocurrent and 0.17, 0.02 and 0.24 for countercurrent. However, both the CO_2 concentrations (co/counter currents) are much lower than carbon capture strategies for having high CO_2 purity above 95%. Permeate purity is important to decrease captured CO_2 transportation cost toward sequestration site.

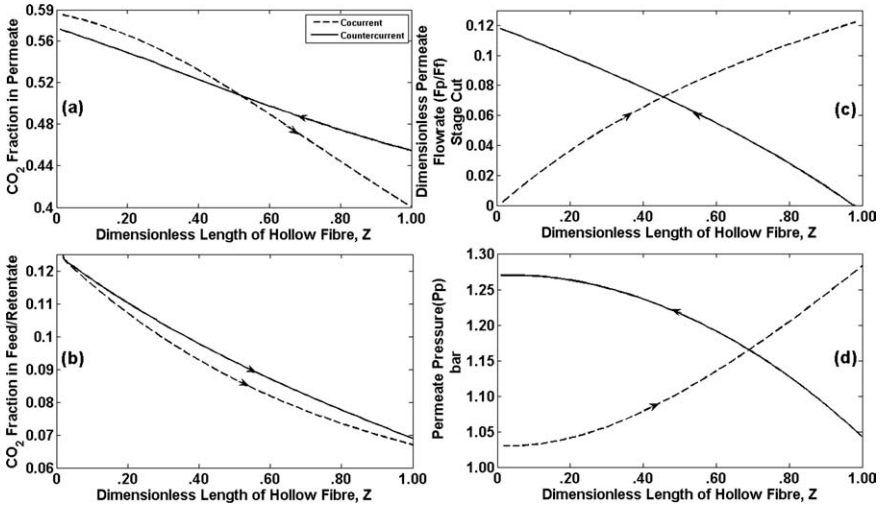

Figure 2. Program output over membrane length at specific feed conditions of $T = 50\ ^{\circ}C$, $P_{f0} = 10$ bar, $P_{p0} = 1.01$ bar, membrane area of 40 m^2/(mol/s), concentrations, mol %: $CO_2 = 13.0$, $N_2 = 80.4$, $O_2 = 3.6$ and $H_2O = 3.0$ and permeance (10^{-10} mol/s.m^2.Pa): $CO_2 = 510$, $N_2 = 10.2$, $O_2 = 25.5$ and $H_2O = 1020$.

(a) CO_2 fraction in permeate, (b) CO_2 fraction in feed/retentate, (c) dimensionless permeate flow rate (stage cut), and (d) permeate pressure.

Figure 2b illustrates the CO_2 concentration (molar fraction) in feed/retentate for the cocurrent and countercurrent flows. As noticed, at the specified operation condition, the membrane can reduce the CO_2 concentration of flue gas from its original value of 0.13 down to about 0.067 and 0.069 for cocurrent and countercurrent, respectively. These values mean that the retentate which will be vented to atmosphere still has notable amount of CO_2.

Figure 2c shows the dimensionless permeate flow rate (stage-cut) profile over the membrane length for both cocurrent and countercurrent flows. According to this figure, in cocurrent arrangement, slightly more flow can penetrate across the membrane (0.122 vs. 0.118).

The feed pressure for both cocurrent and countercurrent flow patterns is a constant value of 10 bars over membrane length. Figure 2d shows permeate pressure over membrane length. Permeate pressures profiles for cocurrent and countercurrent have opposite patterns due to different permeate flow directions. The pressure is atmospheric for both the flow patterns at permeate start point. As noticed, the output permeate pressures are almost similar and to be more precise, cocurrent flow has slightly higher pressure (1.287 bar vs. 1.270 bar).

The recovery is defined as proportion of CO_2 in outlet permeate against inlet feed and is given by

$$Rc = \frac{y_{i,J} F_{p,J}}{x_{i,0} F_{f,0}} \tag{11}$$

The CO_2 recovery for the aforementioned calculation is found to be 37.6% and 41.3% for cocurrent and countercurrent flows, respectively, recalling that current carbon capture recovery targets are in the order of 90%. This has shown that membrane separation was not successful to capture acceptable amounts of CO_2 at the operating condition used with flue gas pressurization to 10 bars. As outlined earlier, a few studies in recent years have highlighted the economic advantage of vacuum mode of operation of membrane separation over pressurized one. In the next calculation, we keep the permeate side at vacuum condition (in contrast with the previous scenario being at atmospheric condition). The main question here is what downstream vacuum pressure would be appropriate? In the few available studies values of 0.03 bar,[37] 0.08 bar,[29] and 0.2 bar[14] have been practiced. However, we agree with Merkel et al.[14] who suggest that although the lowest vacuum pressure is desired, for large-scale industrial application such as carbon capture from power plants, vacuum pressure lower than 0.2 bar might not be practical if one is to consider the structure limitation of membrane material. For this reason we implement 0.2 bar in this study.

We use input feed pressure of 2.0 bar, to fix the feed and permeate pressure proportion at 10 similar to that of previous scenario. Therefore, in this scenario, all the parameters are exactly the same as before (even pressure ratios) except that the previous was pressurized process and this one is *in vacuo*. Figure 3 illustrates the solution output for this scenario.

According to Figure 3a, the CO_2 concentration in permeate is 0.47 and 0.55 for co/counter current flows, respectively. These values are relatively higher than pressurized scenario. Figure 3b illustrates the concentration profile of feed/retentate. At the fiber outlet, CO_2 concentration is 0.116 and 0.117 for co/counter current flows, respectively.

The stage-cut profile is illustrated in Figure 3c. According to this figure, only 2.8% (co), and 2.4% (counter) of feed flue gas can penetrate across the membrane. These values are much lower than those of the pressurized scenario, being about one-fifth. The outlet permeate pressures for co- and countercurrent flows, according to Figure 3d are 0.42 and 0.36 bar, respectively.

The total CO_2 recovery is calculated to be 10.0% and 9.9% for co/counter current flows, respectively. These values are much lower than those for pressurized scenario (ca. one-fourth). Recalling Eq. 2, the key mass-transfer influential parameters are permeance, membrane area and feed

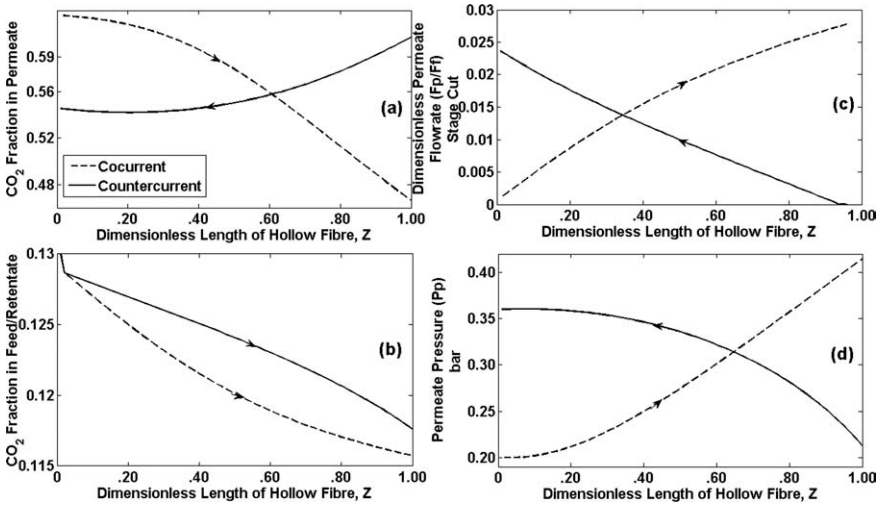

Figure 3. Program output over membrane length at specific feed conditions of $T = 50\ ^{\circ}C$, $P_{f0} = 2.0$ bar, $P_{p0} = 0.2$ bar, membrane area of 40 m^2/(mol/s), concentrations, mol %: $CO_2 = 13.0$, $N_2 = 80.4$, $O_2 = 3.6$ and $H_2O = 3.0$ and permeance (10^{-10} mol/s.m^2.Pa): $CO_2 = 510$, $N_2 = 10.2$, $O_2 = 25.5$ and $H_2O = 1020$.

(a) CO_2 fraction in permeate, (b) CO_2 fraction in feed/retentate, (c) dimensionless permeate flow rate (stage cut), and (d) permeate pressure.

pressure (driving force). With permeance being constant, we can conclude that for the vacuum mode of operation to achieve similar recovery to that of the pressurized mode, it requires either higher pressure ratio or higher membrane area. The pressurization is discarded as the objective of having vacuum process is to prevent the high-compression costs. The area, however, might be the solution, meaning that vacuum process will require high membrane area. Therefore, the appropriateness of vacuum mode of operation, whether for carbon capture or any other membrane gas separation system, lies in the trade-off between energy costs and membrane material costs. Therefore, detailed technoeconomical analyses are warranted for this. We can only project that with growing energy price and with development of new high-efficiency and low-cost membranes, the vacuum process might be the choice in the future. In the next section, we investigate the impact of various parameters on membrane performance including both vacuum and pressurized scenarios.

Parametric Analysis

Membrane separation performance, according to Eq. 2 and as discussed throughout the previous sections, is directly related to permeance, pressure and area. There are other secondary parameters such as selectivity and/or feed concentration, etc., that affect the decision on the application of membranes. In this section, we study the impact of these parameters on membrane performance.

Membrane design

One of the important questions that a membrane manufacturer may encounter is the determination of the required length of a membrane module. We know that membrane area is given by $A = 2\pi R_o LN$. Having A and R_o constant, we have constant value for LN, i.e., the product of length (L) by number of fibers (N). The answer to the design question for a single membrane module can then be either: less number of longer fibers, or larger number of shorter fibers. We have studied this problem with the results shown in Figure 4.

It is noticed that the recovery of CO_2, for both cocurrent and countercurrent flows, decreases with increase of membrane length. It is also noticed that CO_2 purity of permeate notably decreases for cocurrent flow but slightly increases for countercurrent flow. For example, at membrane length of 0.5 m the purity for cocurrent and countercurrent flows are very similar (being 0.6036 and 0.6038, respectively). However, at membrane length of 2.5 m the values become 0.42 and 0.61, respectively. This implies that for cocurrent flow, shorter length is beneficial both for purity and recovery. For countercurrent flow, although length has different impacts on purity (positive), and recovery (negative), the impact on recovery looks stronger than that of purity. This means that for a membrane with fixed area of A it is more advantageous to have shorter length resulting in higher number of fibers. This may be reasoned that shorter length helps purity of CO_2 remain higher (only for cocurrent). Furthermore, design with more fibres takes care of stage-cut resulting in higher recovery. It should, however, be noted that the decision on what length to choose is related to manufacturing limitations as lengths below certain limits might not be practical. The cost of module size is another consideration in such decisions. The immediate estimation is that small-length strategy will increase the total number of installed modules and, thus, capex, but due to higher recovery will reduce opex.

Another observation from Figure 4b is that up to a certain membrane length, cocurrent flow results in higher recovery after which countercurrent shows advantage. In the aforemnetioned example, under the given condition, the threshold length is 0.9 m.

Impact of feed quality

Feed quality is a very definitive process selection and design parameter. Figure 5 illustrates the impact of CO_2 concentration of feed flue gas on permeate purity. As noticed in Figure 5, when the concentration of CO_2 in the feed increases,

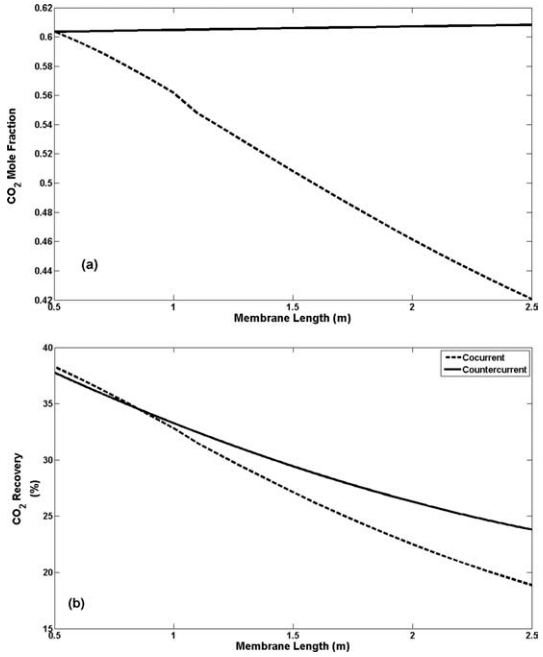

Figure 4. Impact of fiber length on membrane performance (a) CO_2 purity, and (b) CO_2 recovery, when $LN = 8 \times 10^5$ and $R_o = 150 \times 10^{-6}$ (identical membrane area of 7.5 m^2/(mol/s)) at specific feed conditions of $T = 50^{\circ}C$, $P_{f0} = 20$ bar, $P_{p0} = 1.01$ bar, concentrations, mol %: $CO_2 = 13.0$, $N_2 = 80.4$, $O_2 = 3.6$ and $H_2O = 3.0$ and permeance (10^{-10} mol/s.m^2.Pa): $CO_2 = 510$, $N_2 = 10.2$, $O_2 = 25.5$ and $H_2O = 1020$.

correspondingly, the purity of permeate increases. For instance, when the concentration of CO_2 in the feed flue gas is 6%, the outlet permeate will have CO_2 purity of 27.6% for cocurrent and 40.5% for countercurrent. However, when the concentration increases to 20% the values will be 61.5% and 72.8% for co/counter, respectively. This upholds the well-known fact that membranes perform efficiently when the concentration of target component is high in the feed.

Flue gases usually have concentrations less than 20% (vol.) and generally about 13–15%. For this reason, membranes will not be a proper choice for carbon capture unless other influencing parameters (to be discussed in the following sections) are correctly selected.

Impact of flue gas pressure and membrane area

Feed pressure and membrane area are two very critical design parameters. High feed pressure translates to higher opex while high membrane area is linked to higher capex. Therefore, it is always desired to have both these values as low as possible. However, any change in these parameters affects the permeate and retentate composition, as well as flow rate and pressure. We study here the impact of these two parameters on membrane performance. We study both pressurized and vacuum conditions. For pressurized scenario (PS) we have studied membrane area in the range of 1.5–15 m^2/(mol/s), and pressure in the range of 2–50 bar. However, the range for vacuum scenario (VS) is 20–200 m^2/(mol/s) for area and 1–5.5 bar for pressure (permeate-side pressure: 0.2 bar).

Permeate pressure. As it is noticed in Figure 6, feed pressure has positive impact on permeate pressure, while the impact of area is reverse. It is also noticed that permeate pressure is less sensitive to membrane area compared with its sensitivity to feed pressure. The trend of membrane profiles for both PS and VS are identical.

Permeate flow Rate. Permeate flow rate has been traditionally addressed with stage-cut ($\theta = F_p/F_{f0}$). High stage-cut is manifestation of high-mass transfer over membrane. As noticed in Figure 7, for both PS and VS, when feed pressure is increased, permeate flow rate and, thus, stage-cut also increase. This can be explained as a result of increasing driving force (Eq. 2) which steadily increases mass transfer over membrane. The membrane area also has similar impact on permeate flow rate. It is noticed that simultaneous increases in both feed pressure and area amplify the increase in the permeate flow rate. For instance, for PS, at area of 1.5 m^2/(mol/s) and pressure of 4 bar, the value of stage-cut is less than 0.001. If the area is kept constant and the pressure is increased 10-fold to 40 bar, the stage-cut will be 0.043. However, if pressure is kept constant at original value of 4 bars and the area is increased 10-fold, the stage-cut will be 0.009. Now, if both area and pressures are simultaneously elevated 10-fold (15 m^2/(mol/s) and 40 bar), the new stage-cut will be 0.202. This validates that membrane area and feed pressure; both have positive impact on stage-cut. The same trend is noticed for VS.

Permeate Concentration. CO_2 concentration of permeate is the most critical parameter in the design of PCC membrane systems. Membrane design objective is usually either minimum concentration of target component in the retentate or maximum concentration in permeate. This target is accompanied with the requirement of high recovery. For the case of flue gas treatment, retentate quality (CO_2 concentration of vented flue gas) is not the direct objective while CO_2 purity of permeate is very important due to requirements of downstream CO_2 compression and transportation systems. Recovery is also important as it reflect the amount of carbon capture. As discussed earlier, a CO_2 purity of above 95% is usually targeted. Figure 8 illustrates the molar fraction of CO_2 in permeate for PS (Figure 8a), and VS (Figure 8b)

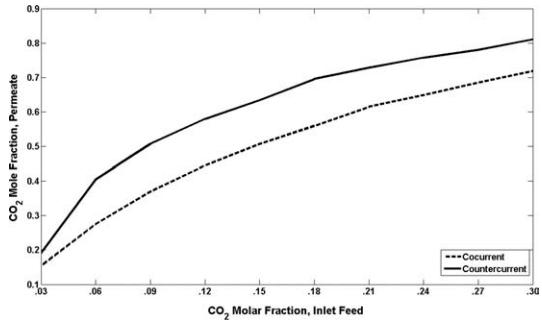

Figure 5. Impact of flue gas composition on permeate concentration of CO_2 at specific feed conditions of $T = 50^{\circ}C$, $P_{f0} = 2$ bar, $P_{p0} = 0.2$ bar, membrane area of 40 m^2/(mol/s), concentrations, mol %: $CO_2 = 13.0$, $N_2 = 80.4$, $O_2 = 3.6$ and $H_2O = 3.0$ and permeance (10^{-10} mol/s.m^2.Pa): $CO_2 = 510$, $N_2 = 10.2$, $O_2 = 25.5$ and $H_2O = 1020$.

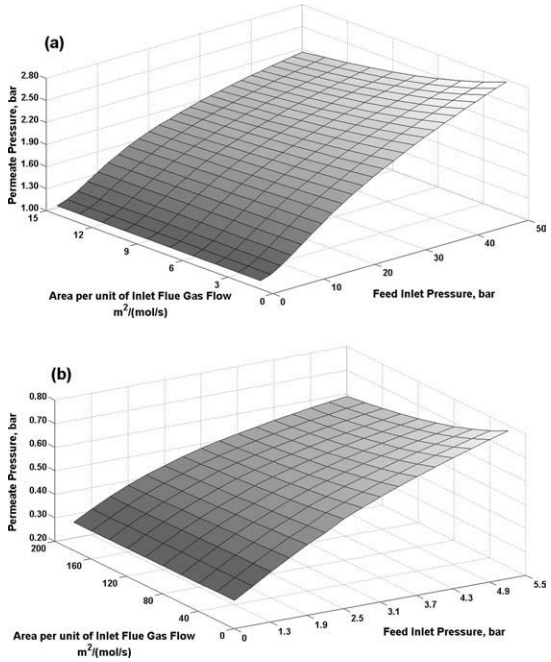

Figure 6. Impact of membrane area and feed pressure on permeate pressure at specific feed conditions of T = 50°C, concentrations, mol %: CO_2 = 13.0, N_2 = 80.4, O_2 = 3.6 and H_2O = 3.0 and permeance (10^{-10} mol/s.m^2.Pa): CO_2 = 510, N_2 = 10.2, O_2 = 25.5 and H_2O = 1020 and cocurrent flow; (a) pressurized P_{p0} = 1.01 bar, and (b) vacuum P_{p0} = 0.20 bar.

processes over wide range of membrane area and inlet flue gas pressure.

It is noticed from both Figure 8a and 8b, that membrane area has reverse impact on CO_2 purity of permeate. The impact becomes more important at high flue gas pressures. The impact of flue gas pressure on permeate purity is seen, however, slightly different. Generally, flue gas pressure has positive impact on CO_2 purity of permeate. This could be easily noticed at relatively low-membrane areas. For instance, for the case of PS, at its low area of 1.5 m^2/(mol/s), the CO_2 purity will be 0.25, 0.60 and 0.65 for flue gas pressures of 2, 10 and 50 bar, respectively. Similarly, at VS's relatively low area of 20 m^2/(mol/s) the CO_2 purity will be 0.43, 0.48 and 0.53 at pressures of 1, 1.9 and 5.5 bar, respectively. However, when the area is increased, CO_2 purity shows a different profile because of two opposite impacts of area and pressure. At higher areas, the increasing trend of purity as a result of pressure increase reaches a maximum at a certain limit after which the reverse impact of area manifests itself in a decline in purity. This is especially noticed for the case of PS, when the profile shows optimal focal. For instance, at high area of 15 m^2/(mol/s), when the feed pressure is 2 bar, the CO_2 purity will be 0.24. It reaches a maximum value of 0.53 at 10 bar after which it declines and reaches a value of 0.18 at 50 bar.

CO_2 Recovery (Captured Carbon). If we consider the stage-cut profiles along with permeate concentration profiles, a trade-off will be observed. Stage-cut becomes maximum at high pressures and areas while CO_2 purity tends to its lowest values at such conditions. Therefore, there is a conflict between our two objectives of maximizing stage-cut as well as CO_2 purity of permeate. We can use "recovery" (Eq. 11) which can manifest the impact of both these parameters on membrane performance. In reality recovery relates to the best combination of stage-cut and purity, but does not necessarily guarantee either of these parameters to be maximum.

Figure 9 shows the recovery profile over area and pressure for PS and VS. It is noticed that the recovery profile for both PS and VS are identical. It is observed that up to certain areas and pressures, increasing both parameters improves the recovery. However, at smaller areas, recovery still improves with increase of pressure, while at higher areas it declines. This means that area above a certain threshold has negative impact on recovery, while below that threshold its influence is positive. These phenomena can be explained by the fact that when area and pressures are increased above certain limit, the driving force of other components (H_2O, N_2 and O_2) also increases and makes negative impact on purity of CO_2, and, thus, recovery. For instance, for the case of PS, at area of 3 m^2/(mol/s), when the pressure is 2 bar, recovery will be 0.03%. The value will steadily elevate till 44.48% at 50 bar. Similarly, at pressure of 10 bar, the recovery will be 3.15% at area of 1.5 m^2/(mol/s) and will steadily elevate to 23.49 till area of 15 m^2/(mol/s). It is, however, noticed that, above a membrane area of 8 m^2/(mol/s), the recovery profile (over pressure) will have declining section. The maximum recovery, is observed to be a 55.3% at area of 8 m^2/(mol/s) and pressure of 50 bar.

The behavior of permeate purity (Figure 8), and recovery (Figure 9), having clear optima, is an interesting outcome that to the best of our knowledge has not been discussed in

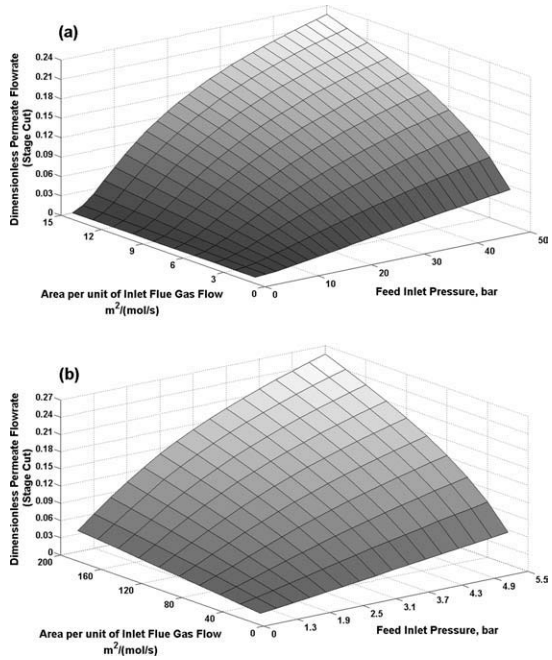

Figure 7. Impact of membrane area and feed pressure on permeate flow rate (stage cut) at specific feed conditions of T = 50°C, concentrations, mol %: CO_2 = 13.0, N_2 = 80.4, O_2 = 3.6 and H_2O = 3.0 and permeance (10^{-10} mol/s.m^2.Pa): CO_2 = 510, N_2 = 10.2, O_2 = 25.5 and H_2O = 1020 and cocurrent flow; (a) pressurized P_{p0} = 1.01 bar, and (b) vacuum P_{p0} = 0.20 bar.

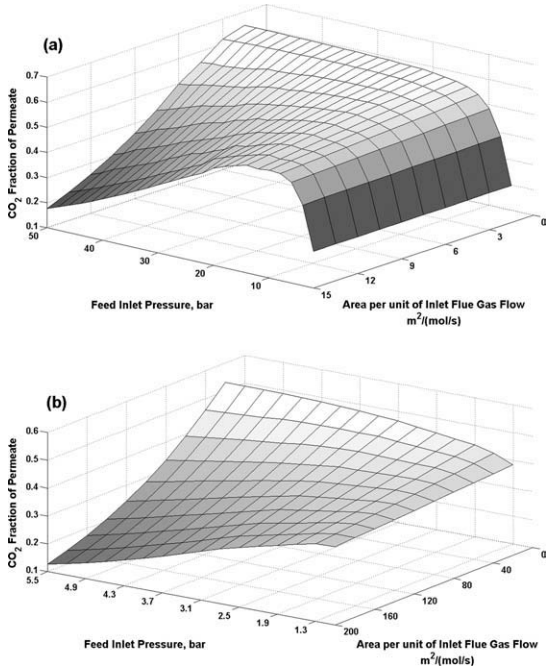

Figure 8. Impact of membrane area and feed pressure on permeate molar fraction of CO_2 at T = 50°C, concentrations, mol %: CO_2 = 13.0, N_2 = 80.4, O_2 = 3.6 and H_2O = 3.0 and permeance (10^{-10} mol/s.m^2.Pa): CO_2 = 510, N_2 = 10.2, O_2 = 25.5 and H_2O = 1020 and cocurrent flow; (a) pressurized P_{p0} = 1.01 bar, and (b) vacuum P_{p0} = 0.20 bar.

literature. These figures propose optimal combinations of feed gas compression pressure and area which could be invaluable outcome for membrane process design. For example, when our objective is maximum recovery, then Figure 9 suggests designing our process in two regions: A and B shown in Figure 10. Region A encompasses the condition with moderate flue gas pressure but high membrane area, while region B is for high-pressure flue gas and moderate area. The decision on choosing either of these regions is dependent on economics of the process. Region A is suitable for the cases when membrane price per unit is low and/or low-compression cost (opex) is targeted. Region B implies very high opex due to high-flue gas compression required and is only good for the condition when membrane material cost is very high.

It should be, however, noted that if there is a certain limit for CO_2 purity of permeate then a different decision is required. Recovery has direct functionality to CO_2 purity of permeate but this does not guarantee that purity will be high. Hence, zones A and B justify optimal recovery at the given condition, but do not take care of purity limits. Therefore, this trade-off should be carefully tailored in membrane system design. When higher purity permeate is required then recovery should be sacrificed. This means that a combination of pressure and area outside zones A and B will be selected which will result at higher process cost.

Assume a design scenario at which the objective is CO_2 purity above 0.5 and maximum recovery. The procedure under such conditions will be first to cross out part of the plane in Figure 10 that related to CO_2 purities below 0.5 (obtained from Figure 8). If all or part of zones A or B still remain, then the parameters will be selected from those zones, else the other points with highest recovery values will be selected.

Impact of permeance and selectivity

Real Selectivity. Selectivity is the most definitive property of membrane material in relation to membrane process design. We know that two different selectivities are defined for membranes. One is the so-called "ideal" selectivity which is obtained by dividing the permeance or permeability values (from experimental data), of fast penetrating component (CO_2) over the less penetrating one (N_2). For our case study the ideal CO_2/N_2 selectivity is 50. However, in reality selectivity is changing when feed stream has multiple components due to competitive penetration between the components. Operating conditions (P, T) also have impact on selectivities. Therefore, the so-called "real" selectivity for the two components is given by

$$\alpha^{r}_{A,B} = \frac{y_A/x_A}{y_B/x_B} \tag{12}$$

Figure 11 illustrates the real selectivity values of CO_2/N_2 under wide ranges of feed pressure and membrane area. Real selectivity is shown to always be less than ideal selectivity (50). At any constant feed pressure, real selectivity decreases steadily with membrane area increase. However, feed pressure seems to have a positive impact on selectivity. Therefore, these two parameters have opposite impacts on selectivity which results in the existence of an optimum condition. This trend is valid for both PS and VS. For instance, at membrane area of 20 m^2/(mol/s) and pressure of 1.3 bar, real selectivity is 7.3. At the same membrane area, increasing the feed pressure

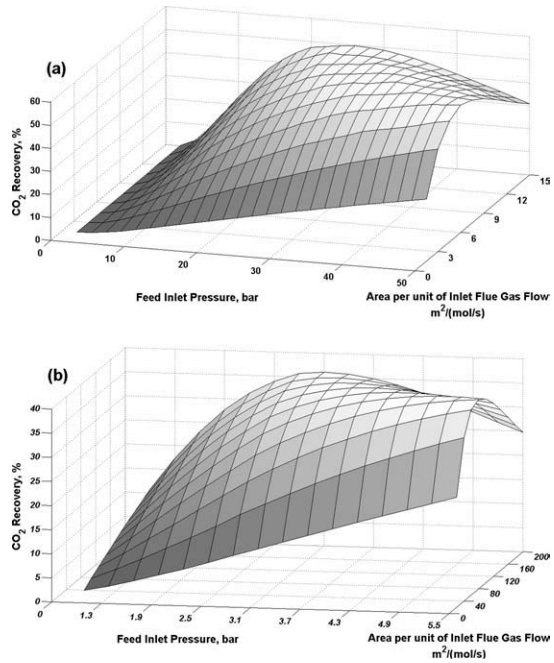

Figure 9. Impact of membrane area and feed pressure on CO_2 recovery at T = 50°C, concentrations, mol %: CO_2 = 13.0, N_2 = 80.4, O_2 = 3.6 and H_2O = 3.0 and permeance (10^{-10} mol/s.m^2.Pa): CO_2 = 510, N_2 = 10.2, O_2 = 25.5 and H_2O = 1020 and cocurrent flow; (a) pressurized P_p0 = 1.01 bar, and (b) vacuum P_{p0} = 0.20 bar.

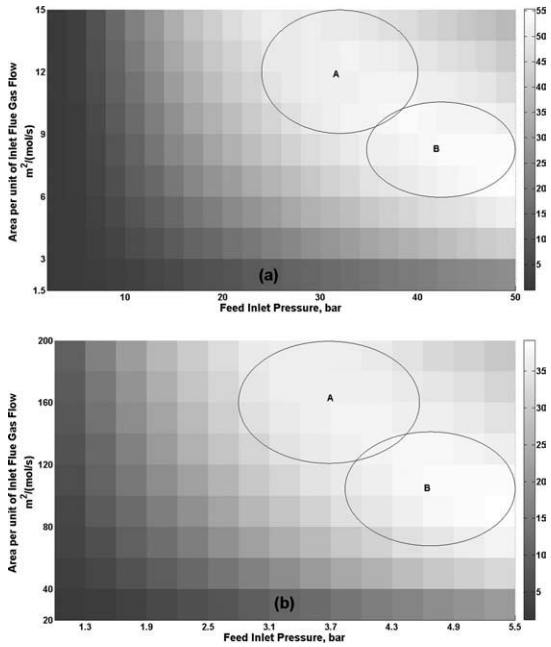

Figure 10. Optimal recovery zones at $T = 50^{\circ}C$, concentrations, mol %: CO_2 = 13.0, N_2 = 80.4, O_2 = 3.6 and H_2O = 3.0 and permeance (10^{-10} mol/s.m^2.Pa): CO_2 = 510, N_2 = 10.2, O_2 = 25.5 and H_2O = 1020 and cocurrent flow; (a) pressurized P_{p0} = 1.01 bar, and (b) vacuum P_{p0} = 0.20 bar.

to 2.5 bar, increases the selectivity to 9.9, and further increasing the pressure to 5.5 bar, improves selectivity to value of 13.7. However, at higher membrane areas the real selectivity values are lower compared to low areas. At an area of 200 m^2/(mol/s), for example, the maximum selectivity is reached at a pressure of 5.5 bar to be 9.3, which is about 32% less compared to that of area 20 m^2/(mol/s).

A similar trend is seen for PS with a difference that the real selectivity values for PS are much higher than those of VS. According to Figure 11, the maximum selectivity for VS is about 13.7 while for PS it is 32.6.

Permeance and Selectivity. It is known that high permeance and selectivity behave against each other. To quantitatively investigate this issue we have kept the membrane area, feed pressure and composition constant and have simulated the process over wide ranges of selectivities and permeances. Figure 12 illustrates the impact of permeance and selectivity on (a) CO_2 concentration, (b) stage-cut, and (c) recovery of permeate for VS.

As noticed, when permeance increases, for a membrane with constant selectivity, the purity of CO_2 in the permeate notably decreases. For instance, permeate CO_2 purity for a membrane with CO_2/N_2 ideal selectivity of 30 will be 0.5 at CO_2 permeance of 100×10^{-10} mol/s.m^2.Pa, while it will be only 0.3 for permeance of $1{,}000 \times 10^{-10}$ mol/s.m^2.Pa. This is because of a higher chance of other components (N_2, O_2) penetrating at high permeances. However, the advantage of high permeance is for achieving higher stage-cut. At the discussed condition, for permeance of 100×10^{-10} mol/s.m^2.Pa, the stage-cut will be 0.02, while for $1{,}000 \times 10^{-10}$ mol/s.m^2.Pa the value will elevate to 0.11.

The impact of selectivity is opposite to that of permeance. At a constant permeance, CO_2 purity increases with increase of selectivity while stage-cut decreases. It is also noticed in Figure 12b that the impact of selectivity on stage-cut is severe at low selectivities, i.e., below ~70.

The combined impact of stage-cut and purity is shown in the recovery profile of Figure 12c. It is noticed that recovery increases with an increase of permeance and decreases with an increase of selectivity. The main insight of this profile is that recovery does not notably change above certain permeance and selectivity values. For instance, we can highlight selectivity values below ~70, and permeance values below $\sim 1{,}000 \times 10^{-10}$ mol/s.m^2.Pa as ranges with notable impact on recovery.

At low permeances, although the membrane separation produces comparatively high purity product, the recovery is low. Conversely, high permeance and low selectivity have high recovery, but with the drawback of low purity. However, in the ranges of medium/high permeance and medium/high selectivity, the membrane separation can produce product with medium purity and medium recovery. As usually from the membrane synthesis point of view, manufacturing high-selective membranes comes with difficulties and expense, and considering that medium selectivity membranes can satisfy similar objectives, we propose that except for cases where either high recovery or high purity is specifically targeted, membranes with medium selectivity and medium/high permeance are adequate choices for CO_2 separation. This region is highlighted with dashed ellipse in Figure 13. This result criticizes the general consensus with stringent focus on designing high selectivity membranes. It

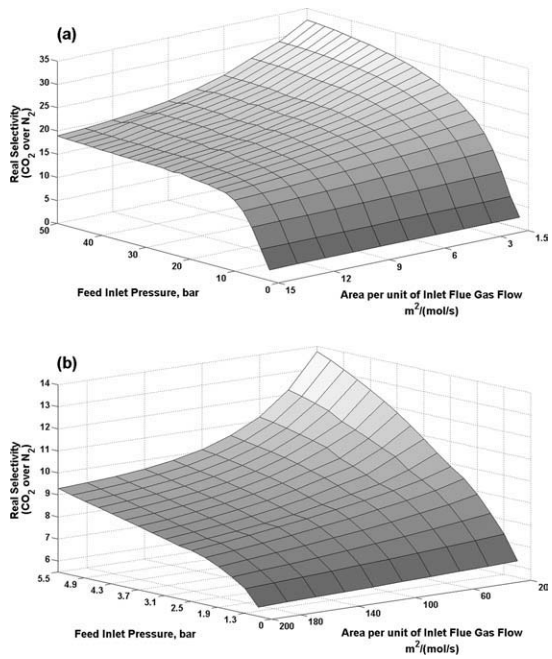

Figure 11. Impact of membrane area and feed pressure on real selectivity of membrane at $T = 50^{\circ}C$, concentrations, mol %: CO_2 = 13.0, N_2 = 80.4, O_2 = 3.6 and H_2O = 3.0 and permeance (10^{-10} mol/s.m^2.Pa): CO_2 = 510, N_2 = 10.2, O_2 = 25.5 and H_2O = 1020 and cocurrent flow; (a) pressurized P_{p0} = 1.01 bar, and (b) vacuum P_{p0} = 0.20 bar.

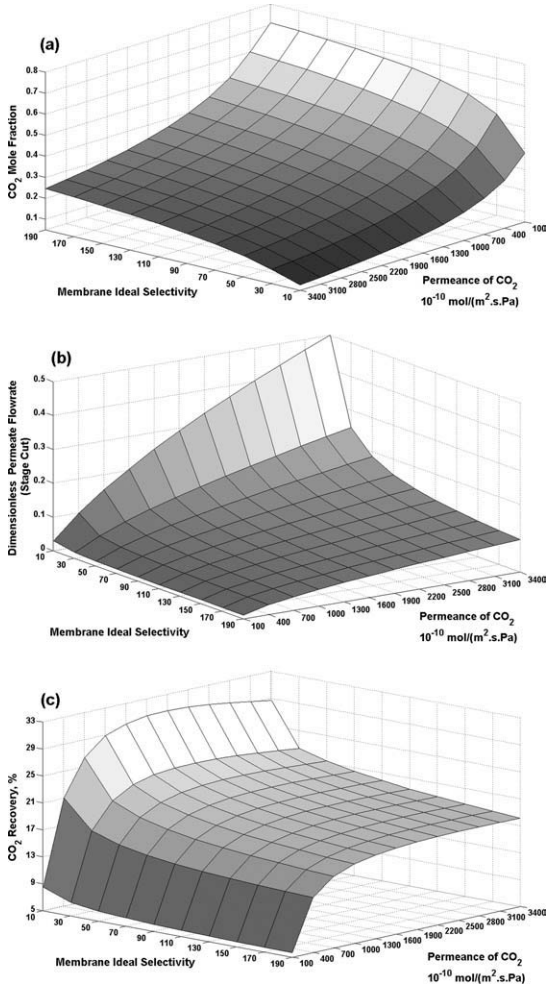

Figure 12. Impact of membrane permeance and selectivity on (a) CO_2 molar fraction of permeate, (b) permeate stage-cut, and (c) CO_2 recovery at $T = 50^{\circ}C$, $P_{f0} = 2.0$ bar, $P_{p0} = 0.2$ bar, membrane area of 80 m^2/(mol/s), concentrations, mol %: $CO_2 = 13.0$, $N_2 = 80.4$, $O_2 = 3.6$ and $H_2O = 3.0$ and, cocurrent flow pattern.

might be advisable that researchers and manufacturers focus on producing membranes with good permeances (as high as $1{,}000 \times 10^{-10}$ mol/s.m^2.Pa) while having acceptable selectivity that are not necessarily high.

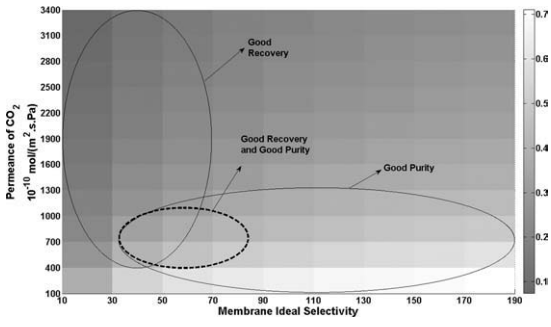

Figure 13. Identification of the right permeance/selectivity values (this figure is two-dimensional (2-D) form of Figure 12a).

Conclusion

n this study, we presented a systematic methodology for analysis of single-stage membrane systems considering multicomponent flue gas with CO_2 as a target component. We found optimal regions of flue gas pressures and membrane area within which a technoeconomical process system design could be carried out. Fiber length was found to be an important parameter in membrane system design having a negative impact on product recovery. We illustrated that the vacuum process requires a notably higher area (i.e., higher capex) than pressurized process, however, the vacuum process was found to be less energy intensive resulting in lower opex.

Throughout the analyses, it was observed that when the concentration of CO_2 in the inlet feed is comparatively low (<15%), membrane separation, neither PS nor VS, can satisfy high-purity permeate or high recovery. The solution to this problem can be afforded by the application of multistage membrane systems, in parallel or series to reach higher qualities. The success of membrane system in carbon capture will be, therefore, very much dependent not only on membrane materials design but also on process synthesis, configuration and optimal design/operation.

The systematic MPCC modeling approach presented in this article provides a foundation for rigorous technoeconomic analysis of MPCC processes with more complex multistage membrane configurations. The research community is invited to dwell into this to assist global decision-makers in the field of carbon capture.

Acknowledgments

The authors gratefully acknowledge Delta Electricity's sponsorship of this project.

Notation

R_{in} = lumen radius of hollow fiber, m
R_o = outside radius of hollow fiber, m
R = ideal gas constant
M = molecular weight, g
l = thickness of membrane, m
N = total number of fibers in hollow fiber system
P_f = feed pressure, Pa
P_p = permeate pressure, Pa
P_i = permeability of component i, mol/m.s.Pa
F_f = feed flow rate, mol/s
K_m = permeance, membrane mass transfer coefficient, mol/m2.s.Pa
Z = dimensionless hollow fiber length
T = temperature, K
x = feed-side concentration of component i, mol fraction
y = permeate concentration of component i, mol fraction
C = number of gas components

Subscripts

i = indicator of gas component
k = indicator of gas component
j = indicator of hollow fiber segment
0 = indicator of condition at membrane inlet
b = Indicator of bulk flow

Greek letters

α^*_{AB} = membrane ideal selectivity for component A over B
α^r_{AB} = membrane real selectivity for component A over B
β = ratio of permeate pressure to feed pressure, P_p/P_f
θ = stage cut, ratio of permeate flow to feed flow F_p/F_{f0}
μ_m = viscosity of gas mixture, Pa. s
μ_m = viscosity of gas mixture, Pa.s

Literature Cited

1. Metz B, Davidson O, Coninck HD, Loos M, Meyer L. *IPCC special report on carbon dioxide capture and storage*. Cambridge: Cambridge University Press, for the Intergovernmental Panel on Climate Change; 2005.
2. Thomas DC, Benson S. *Carbon Dioxide Capture for Storage in Deep Geologic Formations: Results from the CO2 Capture Project*. 1st ed. Amsterdam; Boston: Elsevier; 2005;2(5):1331.
3. Wilson EJ, Gerard D. *Carbon Capture and Sequestration : Integrating Technology, Monitoring and Regulation*. Ames, Iowa: Blackwell Publishing; 2007.
4. Deutch JM, Moniz EJ.*Summary for Policy Makers*. In: *Retro-Fitting of Coal-Fired Power Plants for CO2 Emissions Reductions Symposium*. Massachusetts Institute of Technology; 2009.
5. Khalilpour R, Abbas A. HEN optimization for efficient retrofitting of coal-fired power plants with post-combustion carbon capture. *Int J Greenhouse Gas Contr*. 2011;5:189–99
6. Gomes VG, Yee KWK. Pressure swing adsorption for carbon dioxide sequestration from exhaust gases. *Sep Purif Technol*. 2002;28:161–71.
7. Ho MT, Allinson GW, Wiley DE. Reducing the cost of CO2 capture from flue gases using pressure swing adsorption. *Ind Eng Chem Res*. 2008;47:4883–90.
8. Zevenhoven R, Fagerlund JICSEES. CO2 fixation by mineral matter; the potential of different mineralization routes. IOP Conferance Ser: Earth Environmental Science; 2009:6.
9. Seader JD, Henley EJ. *Separation Process Principles*. Hoboken, NJ: John Wiley &Sons; 2006:34.
10. Ettouneya HM, Al-Enezia G, Hughesa R. Modelling of enrichment of natural gas wells by membranes *Gas Sep Purif*. 1995;9:3–11
11. Baker RW, Lokhandwala K. Natural gas processing with membranes: An overview. *Ind Eng Chem Res*. 2008;47:2109–21.
12. Kawakami M, Iwanaga H, Hara Y, Iwamoto M, Kagawa S. Gas permeabilities of cellulose nitrate poly(ethylene glycol) blend membranes. *J Appl Polym Sci*. 1982;27:2387–93.
13. Powell CE, Qiao GG. Polymeric CO2/N-2 gas separation membranes for the capture of carbon dioxide from power plant flue gases. *J Membr Sci*. 2006;279:1–49.
14. Merkel TC, Lin H, Wei X, Baker R. Power plant post-combustion carbon dioxide capture: An opportunity for membranes. *J Membr Sci*. 2010;359:126–139.
15. Scholes CA, Stevens GW, Kentish SE. The effect of hydrogen sulfide, carbon monoxide and water on the performance of a PDMS membrane in carbon dioxide/nitrogen separation. *J Membr Sci*. 2010;350:189–99.
16. Sada E, Kumazawa H, Wang JS, Koizumi M. Separation of carbon-dioxide by asymmetric hollow fiber membrane of cellulose triacetate. *J Appl Polym Sci*. 1992;45:2181–6.
17. Scholes C, Kentish S, Stevens G. Effects of minor components in carbon dioxide capture using polymeric gas separation membranes. *Sep Purif Rev*. 2009;38:1–44.
18. Koros WJ, Fleming GK. Membrane-based gas separation. *J Membr Sci*. 1993;83:1–80.
19. Vandersluijs JP, Hendriks CA, Blok K. Feasibility of polymer membranes for carbon-dioxide recovery from flue-gases. *Energy Convers Manage*. 1992;33:429–36.
20. Feron PHM, Jansen AE, Klaassen R. Membrane technology in carbon-dioxide removal. *Energy Conver Manage*. 1992;33:421–8.
21. Favre E. Carbon dioxide recovery from post-combustion processes: Can gas permeation membranes compete with absorption? *J Membr Sci*. 2007;294:50–9.
22. Aresta M.*Carbon Dioxide Recovery and Utilization. Dordrecht*; Boston: Kluwer Academic Publishers; 2003:21.
23. Wolsky AM, Daniels EJ, Jody BJ. CO_2 Capture from the flue-gas of conventional fossil-fuel-fired power-plants. *Environ Progr*. 1994;13:214–9.
24. Kazama S, Morimoto S, Tanaka S, Mano H, Yashima T, Yamada K, Haraya K. Cardo Polyimide Membranes for CO_2 Capture from Flue Gases, Greenhouse Gas Control Technologies. In: *7th International Conference on Greenhouse Gas Control Technologies*. Vancouver, Canada; 2004.
25. Matsumiya N, Teramoto M, Kitada S, Matsuyama H. Evaluation of energy consumption for separation of CO_2 in flue gas by hollow fiber facilitated transport membrane module with permeation of amine solution. *Sep Purif Technol*. 2005;46:26–32.
26. Bounaceur R, Lape N, Roizard D, Vallieres C, Favre E. Membrane processes for post-combustion carbon dioxide capture: A parametric study. *Energy*. 2006;31:2556–70.
27. Ho MT, Leamon G, Allinson GW, Wiley DE. Economics of CO2 and mixed gas geosequestration of flue gas using gas separation membranes. *Ind Eng Chem Res*. 2006;45:2546–52.
28. Ho MT, Allinson G, Wiley DE. Comparison of CO2 separation options for geo-sequestration: are membranes competitive? *Desalination*. 2006;192:288–95.
29. Ho MT, Allinson GW, Wiley DE. Reducing the cost of CO2 capture from flue gases using membrane technology. *Ind Eng Chem Res*. 2008;47:1562–8.
30. Bernardo P, Drioli E, Golemme G. Membrane gas separation: A review/state of the art. *Ind Eng Chem Res*. 2009;48:4638–63.
31. Khalilpour R, Abbas A, Lai Z, Pinnau I.*Membrane Systems Engineering: Modeling Hollow Fiber Membranes for Multicomponent Gas Separation*. Australia: The University of Sydney; 2011.
32. Geankoplis CJ.*Transport Processes and Unit Operations*. Engelwood Cliffs, NJ: PTR Prentice Hall; 1993:13.
33. Shindo Y, Hakuta T, Yoshitome H, Inoue H. Calculation methods for multicomponent gas separation by permeation. *Sep Sci Technol*. 1985;20:445–59.
34. Pan CY. Gas separation by high-flux, asymmetric hollow-fiber membrane. *AIChE J*. 1986;32:2020–7.
35. McCabe WL, Smith JC, Harriott P.*Unit Operations of Chemical Engineering*. Boston: McGraw-Hill; 2005:25.
36. Wilke CR. A viscosity equation for gas mixtures. *J Chem Phys*. 1950;18:517–9.
37. Zhao L, Riensche E, Menzer R, Blum L, Stolten D. A parametric study of CO2/N-2 gas separation membrane processes for post-combustion capture. *J Membr Sci*. 2008;325:284–94.

Manuscript received Dec. 8, 2010, revision received Apr. 26, 2011, and final revision received Jun. 1, 2011.